Reliability-Based Design for the Serviceability Limit State of Axially-Loaded Driven Piles in Ontario Soils

Markus Jesswein & Jinyuan Liu
Department of Civil Engineering – Ryerson University, Toronto, ON, Canada
Minkyung Kwak
Ministry of Transportation of Ontario, Toronto, ON, Canada

ABSTRACT
For steel driven piles subjected to axial loads, this paper presents a simplified reliability-based design (RBD) approach for the allowable load at the serviceability limit state (SLS). First, load-displacement responses were obtained from 40 piles that were located in Ontario, Canada and tested to plunging failure. Second, the measured resistance was interpreted from the test results with the Davisson failure criterion and was used to normalize the load-displacement curves. Conventional design methods determined the capacity with measurements from standard penetration tests (SPT), and their uncertainty was modeled with the capacity bias, a ratio of the measured to predicted capacity. Third, a simple hyperbolic curve was adopted to represent the pile load-displacement responses, and the hyperbolic model parameters were determined through regression. Afterwards, copula theory was adopted to represent the correlation structure of the hyperbolic model, and Monte Carlo simulations computed the reliability of the driven piles at the SLS. High lumped-load capacity factors were obtained for the SLS since the SPT design method predicted the capacity with a significant amount of variability. Since a variety of soil conditions were encountered, the analysis aims to provide greater insight on the reliability of SLS designs.

RÉSUMÉ
Pour les pieux entraînés en acier soumis à des charges axiales, ce document présente une approche de conception basée sur la fiabilité (RBD) simplifiée pour la charge admissible à l'état limite de service (SLS). Premièrement, les réponses au déplacement de charge ont été obtenues à partir de 40 pieux situés en Ontario, au Canada, et testés pour déterminer leur défaillance en plongée. Deuxièmement, la résistance mesurée a été interprétée à partir des résultats du test avec le critère de défaillance de Davisson et a été utilisée pour normaliser les courbes charge-déplacement. Les méthodes de conception conventionnelles déterminaient la capacité à l'aide de mesures issues d'essais de pénétration standard (SPT) et leur incertitude était modélisée avec le biais de capacité, un rapport de la capacité mesurée à la capacité prévue. Troisièmement, une courbe hyperbolique simple a été adoptée pour représenter les réponses de déplacement de charge de pile, et les paramètres du modèle hyperbolique ont été déterminés par régression. Ensuite, la théorie des copules a été adoptée pour représenter la structure de corrélation du modèle hyperbolique et des simulations de Monte Carlo ont calculé la fiabilité des pieux pilotés au niveau du SLS. Des facteurs de capacité de charge forfaitaire élevés ont été obtenus pour le SLS puisque la méthode de conception SPT prédit la capacité avec une variabilité importante. Comme diverses conditions de sol ont été rencontrées, l'analyse vise à fournir un meilleur aperçu de la fiabilité des conceptions SLS.

1 INTRODUCTION

The design of a pile needs to meet two conditions to offer a safe and suitable foundation: 1) the ultimate limit state (ULS) considers the maximum applied load that can be supported; and 2) the serviceability limit state (SLS) considers the deformation of the foundation within a tolerable or prescribed limit. For the ULS, many Load and Resistance Factor Designs (LRFD) have been generated over the last few decades; however, the SLS usually governs a design and has received less attention for the development of reliability-based designs (RBD) (Reddy and Stuedlein 2017; Uzielli and Mayne 2011). Several approaches have been proposed to predict the deformation of piles in either cohesive or cohesionless soils, but these methods may experience variability with heterogenous profiles and soils, such as glacial tills and varved clays or silts. In addition, relationships were usually developed with local soil conditions in various regions of the world. Thus, the goal of this paper is to propose a simplified RBD for axially-loaded driven piles in Ontario soils with standard penetration tests (SPT).

Since a large amount of research has been conducted at ULS (Tang and Phoon 2018a), North America has largely adopted LRFD as the preferred RBD system, in which resistance factors are calibrated from the statistical performance of a capacity design method (AASHTO 2014). In this paper, a reliability analysis was conducted for the pile deformation with a procedure similar to LRFD (Tang and Phoon 2018a), but the pile resistance was replaced with an allowable load that corresponds to a tolerable settlement. First, from the Ministry of Transportation of Ontario (MTO), a database of pile tests was collected with high-quality load-displacement responses and soil measurements. Second, from the load-displacement responses of the piles, the mobilized loads were normalized by the pile resistance that was assessed by a failure criterion. The ability to determine the mobilized load then becomes dependent on the pile capacity, which was predicted with conventional design methods. A hyperbolic model was adopted to represent the load-displacement

response, and the hyperbolic model parameters were determined from nonlinear least squares regression. Third, the hyperbolic model parameters were assessed on their statistical properties, which includes the mean, coefficient of variation (COV), and probability distribution. The correlation structure for the parameters of the load-displacement model was represented with copula theory. Lastly, resistance factors were computed for the SLS with Monte Carlo simulations (MCS) by simulating the load-displacement responses for applied and allowable loads. In all, the analysis demonstrates the application of RBD for pile designs in Ontario soils.

2 PILE LOAD TEST DATABASE

2.1 MTO Database

The pile tests were conducted by MTO between 1954 to 1994 in various regions of Ontario. For this study, the focus was on driven steel piles, particularly pipe and H piles, subjected to static axial-compression loads. Piles were sometimes tested more than once with compression and tension maintained-load tests. For piles tested multiple times, the compressive load test was typically performed first, and the setup time, which is the duration between installing and testing a pile, varied from a week to a month. Short setup times occurred for piles in mainly cohesionless soils, and longer setup times were allowed for piles in cohesive soils. The pile properties, such as the geometry and type, and locations are known from the MTO database.

2.2 Soil Conditions of Test Sites

A variety of soil conditions were encountered from the studied sites. Most sites were located in Southern Ontario and had heterogeneous soil profiles. For example, Site 5 near Marathon contained varved silty clays and clayey silts, while Site 33 near Buttonville had intermittent layers of clayey silts and silty sands. Geotechnical soil conditions from the sites were collected from borehole logs. The borehole logs provided the soil descriptions and SPT N-values.

2.3 Selection of Test Data for the Analysis

The selected data and its attributes will influence the evaluation of model parameters and computation of the reliability index. Similar to Tang and Phoon (2018a), the pile test data selected for the analysis was divided into two categories: usable and reliable. From the database by MTO, reliable data focuses on the load-displacement response from a pile test. The data can be evaluated with the capacity failure methods without extrapolation and determine the parameters for the hyperbolic model. Usable test data required sufficient soil measurements since it was used to determine the pile capacity with design methods.

Reliable data were selected from the first axial-compression test. Since some piles were tested more than once, the first test was selected to reduce the uncertainty and influence of setup times and residual stresses induced from repetitive testing. The reliable pile tests needed to be sufficiently loaded to failure, preferably to plunging failure, to accurately determine the ULS and SLS behaviour. From the field load-displacement responses, the capacity was determined without extrapolation with the Hansen 90 % failure criterion (Fellenius 1980). The Hansen 90 % criterion does not heavily rely on judgement by the user and uses a mathematical relationship to offer consistent assessments (Fellenius 1980). To ensure mobilization at the pile tip, the criterion is known to provide a capacity closer to plunging and greater than most failure methods (Fellenius 1980). From the available 168 pile tests, a total of 40 piles (20 pipe piles; 20 H piles) were selected.

Table 1. Summary of Reliable Pile Properties

Property[1]	Statistic	Pile Type		
		H Piles	Pipe Piles	All
L/D	Min	9.8	9.3	9.3
	Mean	67.5	53.0	60.3
	Max	109.6	111.0	111.0
N_{avg}	Min	4.5	5.0	4.5
	Mean	18.1	17.5	17.8
	Max	48.4	55.4	55.4
Qu_m (kN)	Min	226	110	110
	Mean	1003	741	872
	Max	2755	2443	2755

[1] Measured Capacity according to Davisson method

For the usable tests, a total of 35 piles (17 pipe piles; 18 H piles) were selected. In addition to meeting the requirements for being reliable, usable data requires sufficient soil measurements along the pile length to calculate the pile capacity. In particular, SPT N-values and the corresponding soil type were known from the borehole logs.

Table 1 shows the range of soil and pile properties for the 35 usable pile tests. The embedment lengths (L) ranged from 3 m to 38 m, and the slenderness ratio (L/D, where D is the pile width or diameter) varied from approximately 9 to 111. The sample of pipe and H piles had approximately the same range of dimensions and soil conditions. The pipe piles were closed-ended and filled with concrete, except for two that were open-ended. The outside diameter of the pipe piles was 324 mm, and the H piles were either 310 x 79 or 310 x 110 designations (mm x kg/m). The average corrected SPT N-value (N_{avg}) along the piles ranged from 4.5 to 55. In general, the tested piles have a diverse set of lengths and soil stiffnesses.

3 SERVICEABILITY LIMIT STATE DESIGN

The goal of this paper is to characterize the model uncertainties for the load-settlement behaviour of axially-loaded driven piles in heterogeneous soils in Ontario, Canada. The methodologies applied in this paper are similar to those described and applied by Tang and Phoon (2018a, 2018b) and Reddy and Stuedlein (2017) but are summarized to offer background information. A simple hyperbolic relationship was used in this study to represent the load-displacement response:

$$Q/Qu_m = s/(a + bs) \quad [1]$$

Where Q is the mobilizing load (in kN) at the pile top, s is the settlement (in mm), and a and b are parameters to shape the hyperbolic function. Typically, Q is normalized by the ultimate capacity, Qu_m, which is measured by pile load tests. The dependency of Qu_m means the ability to accurately predict the ULS will be important during design. Equation 1 has provided a good representation of the load-displacement response for many foundation elements, such as driven piles (Tang and Phoon 2018a, 2018b), helical piles (Tang and Phoon 2018c), augered cast-in-place piles (Reddy and Stuedlein 2017), and shallow footings (Uzielli and Mayne 2011). The relationship is preferred since it is simple and the hyperbolic parameters (a and b) have a physical meaning. The initial slope of the pile response is represented by a, while the asymptote of the load or normalized load is represented with b.

In practice, the SLS is exceeded when s from an applied load, Q_{app}, is greater than a prescribed allowable settlement, s_a, which varies depending on the project. The s_a corresponds to an allowable load, Q_a, and failure of the SLS can also then be defined as when Q_{app} is greater than Q_a. Thus, the probability of failure (p_f) for exceeding the SLS is expressed by the following limit state function (Tang and Phoon 2018a):

$$p_f = Pr(Q_a - Q_{app} \leq 0) \quad [2]$$

The symbol Pr represents the probability.

Since the hyperbolic relationship was adopted in Equation 1, Q_a can be approximated by the following:

$$Q_a = s_a/(a + bs_a)Qu_m \quad [3]$$

The uncertainty of predicting the capacity or ULS is usually characterized by the capacity bias, M_u, which is a ratio of Qu_m to the predicted capacity, Qu_p:

$$M_u = Qu_m/Qu_p \quad [4]$$

Qu_m is evaluated by a failure criterion, while Qu_p is calculated by a design method. After combining Equations 2, 3 and 4, the resulting equation is provided for p_f (Tang and Phoon 2018a):

$$p_f = Pr(s_a/(a + bs_a) \leq (1/\psi_q)(Q'/M_u)) \quad [5]$$

Q' is a normalized random variable of the applied load and is a ratio of Q_{app} to the nominal applied load, Q_n. ψ_q is the lumped load-capacity factor and is a ratio of Qu_p to Q_n.

If the limit state function is assumed to be normally distributed, the reliability index, β, can be determined from p_f by applying the inverse standard normal cumulative function, ϕ^{-1} (Reddy and Stuedlein 2017):

$$\beta = -\phi^{-1}(p_f) \quad [6]$$

4 COLLECTION OF MODEL FACTORS

4.1 Introduction to Model Factors

For β to be computed for each ψ_q, Equation 5 requires several model factors, namely M_u and hyperbolic parameters a and b. For a given ψ_q and set of statistical properties for the model factors, β was determined in this study with MCS. MCSs were applied because they are not limited to a single type of statistical distribution, such as normal, lognormal, or Weibull, and are applicable for nonlinear limit state functions (Reddy and Stuedlein 2017).

4.2 Measured Axial Capacity (Qu_m)

The Davisson method determined Qu_m as it is recommended by the American Association of State Highway and Transportation Officials (AASHTO) (2012). The method is a graphical approach. An elastic line was drawn as a function of the pile material stiffness, and the elastic line was offset along the displacement axis. In all, if the following equation intersected the experimental field curve, Qu_m was the load corresponding to the intersection point (Fellenius 1980):

$$s = QL/EA + D/120 + 3.81 \text{ (mm)} \quad [7]$$

Where A is the cross-sectional area of the pile, E is the pile elastic modulus, L is the pile length, and D is the pile width or diameter.

4.3 Predicted Axial Capacity (Qu_p)

For SPT measurements, Qu_p can be calculated with direct or indirect design methods. Direct design methods generally rely on the average SPT N-values to predict the capacity and may not be the most reliable approach for heterogeneous soil conditions. For indirect methods, SPT N-values are used to predict the soil strength parameters, such as the undrained shear strength (Cu) and the friction angle (φ'). The strength parameters are then applied to predict the capacity with approaches based on classical soil mechanics theory. In this study, Qu_p was calculated with indirect design methods for the 35 usable piles tested with compression loads.

For driven piles subject to compression loads, the capacity is generally composed of the side resistance and tip resistance, and it can be expressed by the unit resistances:

$$Qu_p = \Sigma q_s As + q_p Ap \quad [8]$$

Where q_s is the unit side resistance, q_p is the unit tip resistance, As is the side area of the pile, and Ap is the area of the pile base. The changing soil types and measurements were considered by dividing the soil profiles into smaller layers along a pile. H piles and open-ended pipe piles were assumed to be fully plugged.

For cohesive soils, the pile unit resistances were determined by the total stress method:

$$q_s = \alpha Cu \quad [9]$$
$$q_p = N_c Cu \quad [10]$$

α and N_c are an empirical adhesion factor and end bearing resistance factor, respectively. A value of 9 was applied for N_c, while α was determined as suggested by Tomlinson (1957).

For cohesionless soils, q_s was determined as below:

$$q_s = K_f K_o \sigma' \tan\delta \quad [11]$$

Where K_f is installation coefficient, K_o is the lateral earth coefficient at rest, σ' is the effective stress, and δ is the friction angle of the soil-pile interface. As recommended by Tomlinson and Woodward (2008), δ was 55 % of φ' and K_f was 0.75 or 1.0 for H piles and pipe piles, respectively. The bearing capacity factor (N_q) was selected as suggested by Berezantzev et al. (1961) for q_p.

$$q_p = N_q \sigma' \quad [12]$$

Cu for cohesive soils and φ' for cohesionless soils were respectively determined by the empirical relationships by Sowers (1954) and Wolff (1989).

$$Cu = 3.75 N_{60} \quad [13]$$
$$\varphi' = 27.1 + 0.3\, N_{60} - 0.00054\, {N_{60}}^2 \quad [14]$$

The field SPT N-values were corrected to N_{60} for 60 % hammer energy according to the Canadian Geotechnical Society (CGS) (2006).

4.4 Comparison between Measured and Predicted Capacities

The indirect design methods mainly underpredicted Qu_m as shown in Figure 1 and with a mean M_u of 1.07. Most of the underpredictions and variabilities occur with piles in cohesive soils and very dense or gravelly cohesionless soils. In these cases, it is generally difficult to reliably predict the strength parameters with SPT N-values. For piles in either cohesive or cohesionless soils, significant

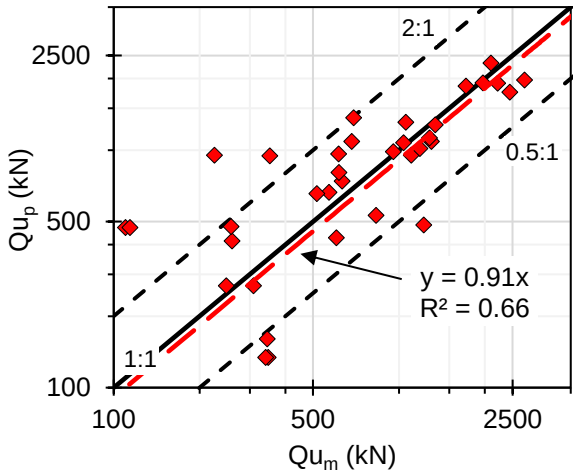

Figure 1. Comparing Measured and Predicted Capacities

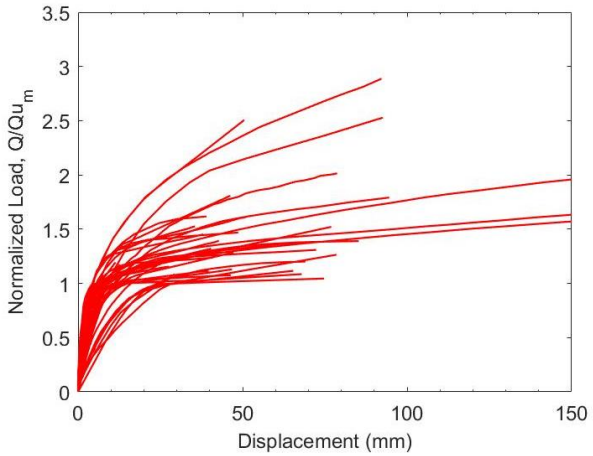

Figure 2. Normalized Load-Displacement Responses

underestimations were found for short piles less than 6 m long. Better predictions were generally obtained with long piles. The investigated design methods do not fully consider the effects of the pile length. For an indirect design approach, the predictions provided moderate variability. The COV of M_u was 56 %, and the coefficient of determination, R^2, was 0.66 between Qu_m and Qu_p.

4.5 Hyperbolic Parameters

For each load-displacement response, Q was normalized by Qu_m that was assessed by the Davisson offset method. In Figure 2, the elastic and plunging slopes on the normalized curves vary due to the different failure mechanisms, pile geometries, and soil conditions. The hyperbolic parameters a and b in Equation 1 were collected for each curve with nonlinear regression.

5 STATISTICAL ANALYSIS OF MODEL FACTORS

5.1 Introduction

During the MCS, the model factors (a, b, and M_u) are simulated by their source probability distributions and should be considered as random variables. The statistical properties of the model factors were investigated for the 40 piles subjected to compression loads. The statistical properties were evaluated by detecting potential outliers; verifying the randomness; collecting descriptive statistics, such as the mean and COV; and fitting probability distributions.

5.2 Detection of Data Outliers

Outliers are values that significantly deviate from the main set of data. Evaluations could provide biased results if outliers were present within the data. Outliers can be visually inspected with the aid of load-displacement plots (Dithinde et al. 2011; Tang and Phoon 2018a). Inspection of Figure 2 does not indicate any potential outliers.

5.3 Verification of Randomness

According to Tang and Phoon (2018a), model factors may be biased by soil or pile properties and should not be immediately represented as random variables. Potentially influential parameters include N_{avg} and L/D (Tang and Phoon 2018a). If a correlation is found between these parameters and a model factor, the model factor can be transformed with a function that represents the statistical dependency. The COV of the transformed model factor can be reduced compared to the non-transformed model factor (Tang and Phoon 2018a). Thus, potential biases should be examined to prevent the development of biases.

Table 2. Results of Spearman Rank-Correlation

Model Factor	n	L/D		N_{avg}	
		r	p-value	r	p-value
a	40	**0.61**	**0.00**	**0.39**	**0.02**
b	40	0.07	0.68	**-0.34**	**0.05**
M_u	35	-0.16	0.35	-0.07	0.70

Note: Bold values indicate a potential correlation with the model factor

Correlations between the model factors and L/D and N_{avg} can be observed with scatter plots, but they can also be assessed with the Spearman rank-correlation test. If the p-value is less than 0.05, the correlation indicated by the coefficient, r, is significantly different from zero and parameter dependence likely exists for a 95 % confidence interval (Howell 2002). For the model factors, Table 2 shows the results of the Spearman rank-correlation test and the number of analyzed samples, n. A fairly strong positive correlation was found between a and L/D with r of 0.61, but a significant correlation was not observed with b or M_u. The p-value was less than 0.05 between N_{avg} and the hyperbolic parameters a and b, but the correlation was ignored as r was low and less than 0.40.

Since a dependency was found between a and L/D, the hyperbolic parameter was transformed to a_t by the following function that was determined empirically:

$$a = a_t \, 1.08 \exp(0.016 \, L/D) \quad [15]$$

According to the Spearman rank test, a_t does not have a dependency with L/D. Other references noticed a correlation between L/D and the hyperbolic parameters and developed empirical functions to transform the model factors (Tang and Phoon 2018b; Reddy and Stuedlein 2017). The functions, such as Equation 15, were obtained by regressing L/D to the hyperbolic parameter, and they vary between the database and foundation type.

5.4 Descriptive Statistics of the Model Factors

Table 3 compares the descriptive statistics of M_u to several references that conducted similar analyses with driven piles under compression loads. The COV of M_u from this study is significantly greater than the other references, but the variability is influenced by the soil conditions, quality of the site investigation techniques, and accuracy of the prediction method. For example, Tang and Phoon (2018a) offered one of the lowest COVs since they relied on cone penetration tests (CPT). In addition, this study combined the piles, regardless of their embedded soil type, but the references usually divided the tests by the soil type.

For the studied piles, the variability of a is higher than the variability of b. The COV was 47 % for a, but the COV was 20 % for b. This trend has been discussed by Tang and Phoon (2018a) and suggests the soil stiffness parameter (a) is associated with more uncertainty than the strength parameter (b). In Table 4, the descriptive statistics of a and b are similar to the results from other publications.

5.5 Fitting of Probability Distributions

In order to conduct MCS, the statistical distributions of the model factors need to be identified. Distributions were considered that assumed the model factors could only possess values greater than zero (positive values), and the goodness-of-fit was conducted with the Anderson-Darling test (Anderson-Darling 1952) at the 95 % confidence interval. M_u, a_t, and b were fitted to a lognormal (with shape parameters μ_{LN} and σ_{LN}), Weibull (with shape parameters α_w and β_w), and Weibull distribution, respectively. Figures 3 to 5 show the fitted distributions offer a reasonable representation of the model factors.

Table 3. Summary of the ULS Model Statistics for Driven Piles Subjected to Compression Loads

Reference	Foundation Type	Soil Type	Design Method[1]	n	Mean	COV (%)
Dithinde et al. (2011)	Driven	Sand	Static formula	28	1.11	33
		Clay	Static formula	59	1.17	26
Tang and Phoon (2018a)	Closed-ended pipe[2]	Sand	ICP-05 method (CPT)	52	1.10	31
			UWA-05 method (CPT)		1.00	39
	Open-ended pipe[2]	Sand	ICP-05 method (CPT)	16	1.07	24
			UWA-05 method (CPT)		1.07	21
Tang and Phoon (2018b)	Steel H	Sand	Nordlund method	46	0.82	47
		Clay	API α method	26	1.10	40
		Layered	API α-Nordlund method	32	0.92	40
This work	Driven steel	All	Tomlinson α-Berezantzev method	35	1.07	56

[1] API, American Petroleum Institute; [2] Concrete-filled steel pile piles

Table 4. Summary of the Descriptive Statistics for the Hyperbolic Parameters for Driven Piles Subjected to Compression Loads

Reference	Foundation Type	Soil Type	n	a[1]		b[1]		ρ_τ[2]
				Mean	COV (%)	Mean	COV (%)	
Dithinde et al. (2011)	Driven	Sand	28	5.55	54	0.71	14	-0.78
		Clay	59	3.58	57	0.78	11	-0.89
Tang and Phoon (2018a)	Closed-ended pipe[3]	Sand	111	6.26	75	0.8	15	-0.56
Tang and Phoon (2018b)	Steel H	Sand	52	1.17	60	0.69	18	-0.60
		Clay	47	1.07	37	1.01	9	-0.51
		Layered	50	1.17	59	0.75	13	-0.53
This work	Driven steel	All	40	1.14	46.7	0.67	19.5	-0.38

[1] Hyperbolic parameters may or may not be transformed by an empirical function; [2] Correlation within hyperbolic parameters, and Dithinde et al. (2011) does not report Kendall tau; [3] Concrete-filled steel pile piles

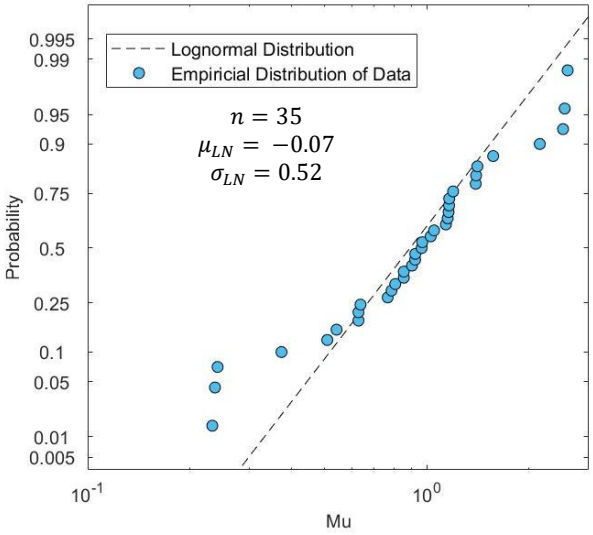

Figure 3. Cumulative Distribution for M_u

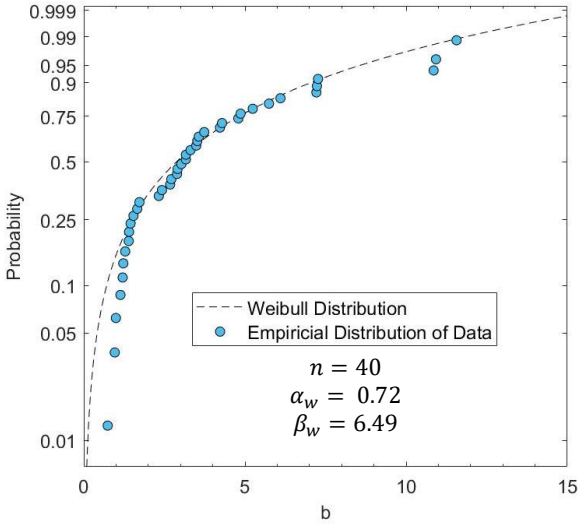

Figure 5. Cumulative Distribution for b

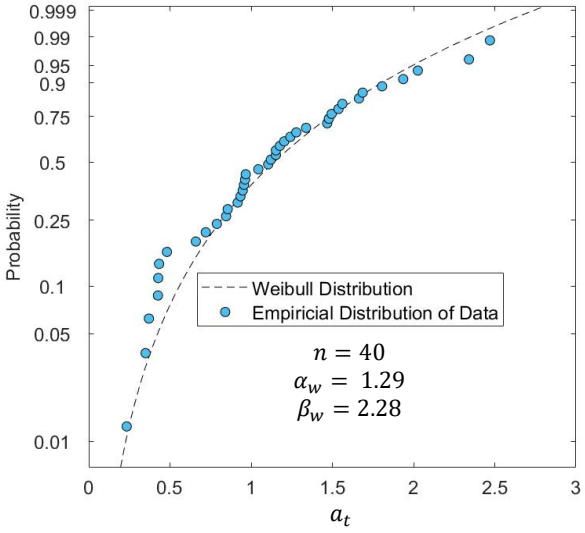

Figure 4. Cumulative Distribution for a_t

5.6 Simulation of Hyperbolic Parameters

Figure 6 shows that the hyperbolic parameters a and b are weakly and inversely correlated. This is confirmed with a Kendall tau coefficient, ρ_τ, of -0.25. However, the correlation was improved between a_t and b with a ρ_τ of -0.38 by considering L/D from Equation 15. Piles with a large tip resistance will likely behave differently than piles with a dominating side resistance, but the trend implies a pile with a stiff elastic response will likely have a slowly decaying plunging slope (Tang and Phoon 2018a).

Copula theory was applied to represent the correlation between parameters a_t and b to avoid the development of a potential bias during the reliability analysis. A similar approach was applied by Tang and Phoon (2018a) and Reddy and Stuedlein (2017). The correlation structure between a_t and b was assumed to fit a Gaussian-type copula. The cumulative probabilities of a_t and b from the fitted distributions were fitted to the copula, and a copula parameter, θ, of -0.52 was obtained.

To verify the fit, the Gaussian copula was used to simulate 1000 pairs of hyperbolic parameters a_t and b. Equation 15 transforms a_t to a to simulate the load-displacement responses. From the database, L/D roughly

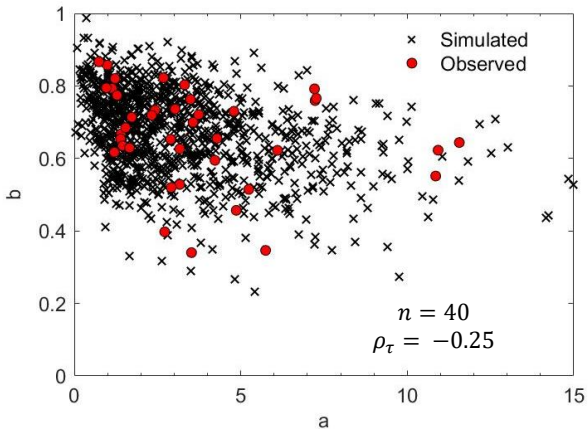

Figure 6. Observed and Simulated Correlation of the Hyperbolic Parameters

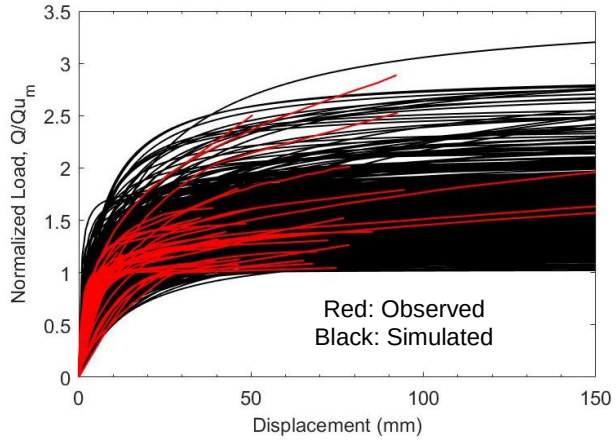

Figure 7. Observed and Simulated Load-Displacement Responses of Piles Subjected to Compression Loads

ranged from 9 to 111. For the simulations, L/D was assumed to range from 8 to 125, which approximately corresponds to a pile length of 3 m to 40 m, with a uniform distribution. Equation 1 then allowed Q to be determined for each set of L/D, a_t, and b. The results of the simulations are shown in Figures 6 and 7. Figure 7 shows the simulated load-displacement responses are within a similar range as the observed responses; thus, the results indicate the copula can satisfactory represent the pile settlement behaviours.

6 CALIBRATION OF LUMPED LOAD-CAPACITY FACTORS

MCS was applied to compute p_f and β from ψ_q. For each ψ_q, five million simulations were generated by randomly sampling variables s_a, Q', M_u, a, and b from their corresponding distributions. If Q_{app} exceeded Q_a as expressed by Equation 5, a failure occurred. The number of failures were summated, and the p_f was then equal to the number of failures divided by the number of simulations.

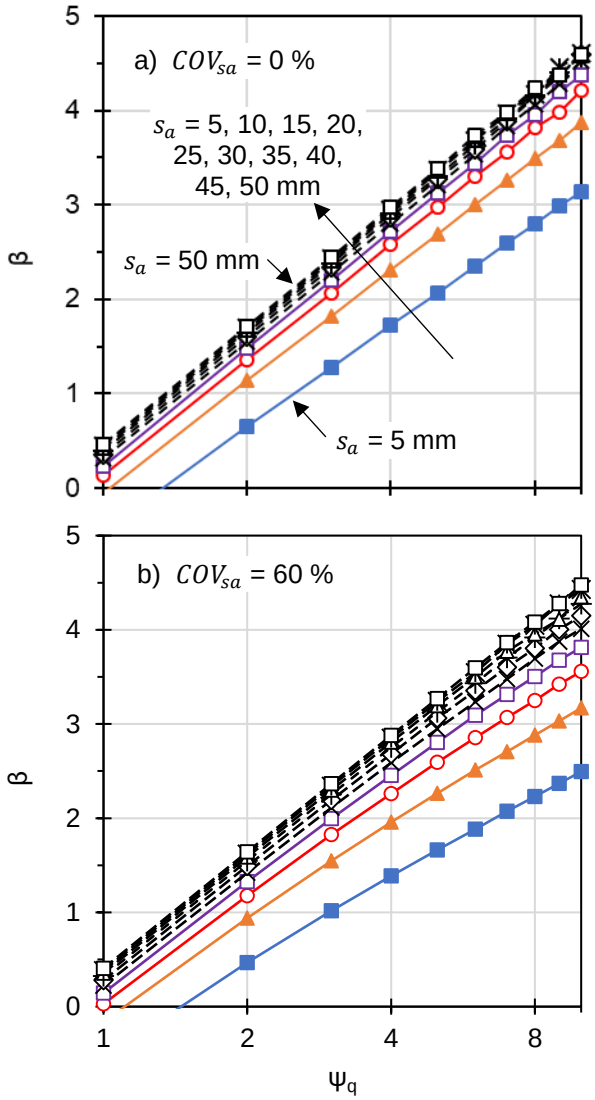

Figure 8. Variation of β with s_a and ψ_q for a) COV_{sa} of 0 % and b) COV_{sa} of 60 %

The uncertainty of s_a is not well characterized; hence, a range of COVs was applied during the computations of β (Uzielli and Mayne 2011). The applied characteristics of s_a was the same as Reddy and Stuedlein (2017) and Tang and Phoon (2018a): s_a was assumed to fit a lognormal distribution; β was determined for each mean s_a, which ranged from 5 mm to 50 mm; and β was also computed for each COV for s_a (COV_{sa}) that ranged from 0 % to 60 %. Q' was also assumed to follow a lognormal distribution with a mean of 1 and a COV of 10 %, which is similar to the inputs for the ULS suggested by AASHTO (2012).

Figure 8 presents β and ψ_q for a COV_{sa} of 0 % and 60 %. The reliability increases as the average s_a increases, but the reliability does not change much between 25 mm to 50 mm. The reliability is slightly influenced by the COV_{sa}, and it decreases as COV_{sa} increases. The large values of ψ_q to obtain a β of 2.33 or 3 indicate a low level of reliability is found overall. This is likely due to the large COV of M_u.

Particularly for cohesive soils, it is difficult to accurately determine the settlement as the design method relies on empirical relationships with SPT N-values.

7 CONCLUSIONS AND DISCUSSIONS

In this study, test results from 35 steel driven piles were used to calculate Qu_p with SPT N-values and an indirect design method for cohesive and cohesionless soils. The indirect design method offered significant variability with cohesive soils and very dense cohesionless soils. The empirical method to estimate C_u likely contributed to the variability, and the capacity was largely underestimated for short piles with a length less than 6 m.

The analysis demonstrates the process to develop a RBD for the SLS, which has been gaining more attention over the last decade. The SLS was simulated by adopting a hyperbolic relationship between the allowable load and settlement. From 40 compression tests, the hyperbolic parameters a and b were collected, and a statistical analysis was conducted to characterize the model factors (M_u, a, and b) based on their descriptive statistics and fitted probability distributions. The dependency between a and b was found to be fairly weak but was simulated with copula theory to prevent potential biases during the analysis. With the source distributions of the model factors, reliability indices were computed for lumped load-capacity factors with MCS. As presented in Figure 8, the large lumped load-capacity factors indicate that the indirect design method lacks accuracy to predict the capacity according to the Davisson criterion. Thus, the ability to reliably determine the load-displacement response is affected. The reliability can be improved by selecting a design method that better considers influences related to the pile length.

The presented analysis was limited by the number of available pile load tests. The piles, regardless of the pile type or embedded soil type, were analyzed together, but differences in load-displacement behaviour will likely exist. Piles in cohesive soils may also be influenced by the soil plasticity, sensitivity, and overconsolidation ratio rather than the SPT N-value. In addition, it should be noted that the reliability will vary by the selected design method and failure criterion.

ACKNOWLEDGEMENTS

The presented research was made possible with funding from the National Sciences and Engineering Research Council of Canada and support and resources provided by the Ministry of Transportation of Ontario. In addition, the authors would like to thank Mr. David Staseff from MTO for sharing the data of pile load tests.

REFERENCES

American Association of State Highway and Transportation Officials (AASHTO). 2012. AASHTO LRFD Bridge Design Specifications, AASHTO, Washington, DC, USA.

Anderson, T.W. and Darling, D.A. 1952. Asymptotic theory of certain goodness-of-fit criteria based on stochastic process, The Annals of Mathematical Statistics, 23(2): 193-212.

Berezantzev, V.G., Khristoforov, V.S., and Golubkov, V. N. 1961. Load bearing capacity and deformation of piled foundations, In Proceedings of the 5th International Conference on Soil Mechanics and Foundation Engineering, 2: 11-15.

Canadian Geotechnical Society (CGS). 2006. *Canadian Foundation Engineering Manual*, 4th ed., CGS, Richmond, BC, Canada.

Dithinde, M., Phoon, K.-K., De Wet, M., and Retief, J.V. 2011. Characterization of model uncertainty in the static pile design formula, *Journal of Geotechnical and Geoenvironmental Engineering*, ASCE, 137(*1*): 70-85.

Fellenius, B.H. 1980. The analysis of results from routine pile load tests, *Ground Engineering*, 13(*6*): 19:31.

Reddy, S.C. and Stuedlein, A.W. 2017. Serviceability limit state reliability-based design of augered cast-in-place piles in granular soils, *Canadian Geotechnical Journal*, 54(*12*): 1704-1715.

Sowers, G. F. 1954. Modern Procedures for Underground Investigations, In Proceedings of the American Society of Civil Engineering, ASCE, 80(435): 1-11.

Tang, C. and Phoon, K.-K. 2018a. Statistics of model factors in reliability-based design of axially loaded driven piles in sand, *Canadian Geotechnical Journal*, 55: 1592-1610.

Tang, C. and Phoon, K.-K. 2018b. Evaluation of model uncertainties in reliability-based design of steel H-piles in axial compression, *Canadian Geotechnical Journal*, 55: 1513-1532.

Tang, C. and Phoon, K.-K. 2018c. Statistics of model factors and consideration in reliability-based design of axially loaded helical piles, *Journal of Geotechnical and Geoenvironmental Engineering*, ASCE, 144(*8*): 04018050-1-17.

Tomlinson, M. J. 1957. The adhesion of piles driven in clay soils, In Proceedings of the 4th International Conference of Soil Mechanics, 2: 66-71.

Tomlinson, M. J. and Woodward, J. 2008. Pile design and construction practice, 5th ed., Taylor and Francis, New York, NY.

Uzielli, M. and Mayne, P.W. 2011. Serviceability limit state CPT-based design for vertically loaded shallow footings on sand, *Geomechanics and Geoengineering*, 6(*2*): 91-97.

Wolff, T. F. 1989. Pile capacity prediction using parameter functions, In Predicted and Observed Axial Behavior of Piles: Results of a Pile Prediction Symposium, ASCE, Geotechnical Special Publication No. 23: 96-106.